An allosteric peptide inhibitor of HIF-1α regulates hypoxia-induced retinal neovascularization

Ayumi Usui-Ouchi[a,b], Edith Aguilar[a], Salome Murinello[a], Mitchell Prins[c], Marin L. Gantner[c], Peter E. Wright[d], Rebecca B. Berlow[d,1], and Martin Friedlander[a,c,1]

[a]Department of Molecular Medicine, The Scripps Research Institute, La Jolla, CA 92037; [b]Department of Ophthalmology, Juntendo University School of Medicine, 113-8421 Tokyo, Japan; [c]Lowy Medical Research Institute, La Jolla, CA 92037; and [d]Department of Integrative Structural and Computational Biology, The Scripps Research Institute, La Jolla, CA 92037

Edited by Jeremy Nathans, The Johns Hopkins University School of Medicine, Baltimore, MD, and approved September 25, 2020 (received for review August 18, 2020)

Retinal neovascularization (NV), a leading cause of vision loss, results from localized hypoxia that stabilizes the hypoxia-inducible transcription factors HIF-1α and HIF-2α, enabling the expression of angiogenic factors and genes required to maintain homeostasis under conditions of oxygen stress. HIF transcriptional activity depends on the interaction between its intrinsically disordered C-terminal domain and the transcriptional coactivators CBP/p300. Much effort is currently directed at disrupting protein–protein interactions between disease-associated transcription factors like HIF and their cellular partners. The intrinsically disordered protein CITED2, a direct product of HIF-mediated transcription, functions as a hypersensitive negative regulator that attenuates the hypoxic response by competing allosterically with HIF-1α for binding to CBP/p300. Here, we show that a peptide fragment of CITED2 is taken up by retinal cells and efficiently regulates pathological angiogenesis in murine models of ischemic retinopathy. Both vaso-obliteration (VO) and NV were significantly inhibited in an oxygen-induced retinopathy (OIR) model following intravitreal injection of the CITED2 peptide. The CITED2 peptide localized to retinal neurons and glia, resulting in decreased expression of HIF target genes. Aflibercept, a commonly used anti-VEGF therapy for retinal neovascular diseases, rescued NV but not VO in OIR. However, a combination of the CITED2 peptide and a reduced dose of aflibercept significantly decreased both NV and VO. In contrast to anti-VEGF agents, the CITED2 peptide can rescue hypoxia-induced retinal NV by modulating the hypoxic response through direct competition with HIF for CBP/p300, suggesting a dual targeting strategy for treatment of ischemic retinal diseases and other neovascular disorders.

HIF inhibition | neovascularization | ischemic retinopathy | combination therapy

The retina requires a continuous supply of oxygen (O_2) and is known as one of the most metabolically active tissues, consuming O_2 more rapidly than even the brain (1, 2). Retinal vascular abnormalities are observed in diabetic retinopathy (DR), retinopathy of prematurity (ROP), and retinal vein occlusion (RVO), leading to ischemia, subsequent hypoxia-induced neovascularization (NV), and fibro(glial)proliferation, which are major causes of vision loss or blindness (3, 4). Historically, patients with proliferative diabetic retinopathy (PDR), advanced stage ROP, or RVO have been treated with retinal photocoagulation to decrease oxygen demand and relieve hypoxia (5, 6). However, retinal photocoagulation can also induce complications such as decreased visual acuity, constriction of visual fields, and diminished night vision due to laser-induced loss of retinal tissue and the retinal pigment epithelium (RPE) (5).

A number of studies have demonstrated the critical role of the proangiogenic cytokine VEGF in development of pathological NV in the eye (7–9). Anti-VEGF drugs have been used clinically to treat choroidal NV and macular edema, as well as hypoxia-induced NV in patients with PDR or ROP (10, 11). While anti-VEGF therapy has dramatically improved our ability to treat these patients, stabilizing or improving visual outcomes in ∼60% of treated patients (12–14), directly targeting VEGF has potential drawbacks; many patients do not respond to VEGF-targeting therapy and those who do may experience negative side effects (15). Furthermore, since the trophic functions of VEGF are critical to maintaining cardiovascular, renal, and nervous tissues including retinal cells and RPE, there are safety concerns associated with repeated intravitreal administration of anti-VEGF therapies in ischemic retinal diseases, especially for diabetic patients or premature babies who are vulnerable to disruption of crucial trophic factors (15). Thus, there is a critical unmet medical need for additional therapeutic strategies for treating ischemic retinal diseases, and specifically hypoxia-induced NV, in the clinic.

One potential alternative therapeutic approach is to target molecules upstream of the VEGF signaling cascade, such as the hypoxia-inducible transcription factor HIF-1α. In the ischemic retina, HIF-1α promotes the expression of VEGF and other angiogenic factors (16). HIF-1α also modulates tissue adaptation to hypoxia by directing the expression of genes involved in glycolysis, homeostasis, angiogenesis, and vasculogenesis (17, 18). One such gene encodes the intrinsically disordered protein CITED2, which functions as a negative feedback regulator of

Significance

Retinal ischemia causes hypoxia-induced neovascularization that stimulates production of proangiogenic cytokines such as VEGF by the hypoxia-inducible transcription factors HIF-1 and HIF-2. Current therapies for ischemic retinal diseases target circulating VEGF but do not modulate the activity of the transcription factors that control its production. We demonstrate that inhibiting HIF-mediated transcription with a peptide derived from the intrinsically disordered protein CITED2, a negative feedback regulator of HIF-1α, reduces pathological angiogenesis in a mouse model of ischemic retinopathy. Combining the CITED2 peptide with the VEGF-Trap aflibercept causes potent suppression of neovascularization and promotes revascularization of the ischemic retina, an outcome not observed for anti-VEGF agents alone, suggesting that dual targeting of the HIF transcription factors and VEGF may be advantageous.

Author contributions: A.U.-O., S.M., M.L.G., R.B.B., and M.F. designed research; A.U.-O., E.A., S.M., M.P., M.L.G., and R.B.B. performed research; A.U.-O., S.M., M.L.G., P.E.W., R.B.B., and M.F. analyzed data; and A.U.-O., M.L.G., P.E.W., R.B.B., and M.F. wrote the paper.

The authors declare no competing interest.

This article is a PNAS Direct Submission.

[1]To whom correspondence may be addressed. Email: rberlow@scripps.edu or friedlan@scripps.edu.

This article contains supporting information online at https://www.pnas.org/lookup/suppl/doi:10.1073/pnas.2017234117/-/DCSupplemental.

First published October 26, 2020.

HIF-1α by competing for binding to the TAZ1 domain of the general transcriptional coactivators CBP and p300 (19, 20). Previously, we reported that a peptide derived from the disordered C-terminal transactivation domain of CITED2 functions allosterically to displace HIF-1α from the TAZ1 domain in vitro, suggesting that it may activate a hypersensitive, unidirectional regulatory switch to efficiently attenuate the hypoxic response in vivo (20). HIF-1α transcriptional activation is directly dependent on interactions between the C-terminal disordered transactivation domain of HIF-1α and TAZ1 (21, 22); inhibition of this interaction could be beneficial for modulating the availability of proangiogenic factors under the control of HIF-1α. Thus, we sought to determine if CITED2 peptides exhibit efficacy as inhibitors of HIF transcriptional activity in vivo and, more specifically, determine whether these peptides could disrupt pathological angiogenesis in the retina.

The oxygen-induced retinopathy (OIR) mouse model of hypoxia-induced NV is a well-established model for investigating putative antiangiogenic compounds (23). Here, we demonstrate that intravitreal injection of a 59-amino acid CITED2 peptide in OIR mice dramatically rescues both hypoxia-induced retinal NV and vaso-obliteration (VO) while also promoting revascularization of the damaged retina. This is in contrast to anti-VEGF therapies, such as aflibercept, that only rescue NV, but not VO, in OIR mice. Our findings suggest that targeting the interaction between HIF-1α and CBP/p300 in the ischemic retina is beneficial not only for inhibiting pathological neovascularization, but also for promoting the normalization of disrupted vasculature. These data indicate that the CITED2 peptide could be useful as a therapeutic agent for the treatment of neovascular eye diseases.

Results

Our previous in vitro studies demonstrated that the CITED2 peptide functions as an allosteric inhibitor of HIF-1α by competing with HIF-1α for binding of the TAZ1 domain of CBP/p300 (20). To investigate whether the CITED2 peptide is able to inhibit HIF-1α in vivo, we used the OIR mouse model of hypoxia-induced retinal NV (23). In the OIR model, the hyperoxic phase from postnatal day 7 (P7) to P12 induces regression of retinal vessels, resulting in an avascular area in the central retina. Returning OIR mice to room air at P12 results in hypoxia relative to the previous 5 d; HIF stabilization in the avascular retina leads to hypoxia-induced retinal NV in the area surrounding the avascular zone, with maximal NV observed at P17 (*SI Appendix*, Fig. S1) (23). OIR mice were injected intravitreally on P12 with three different doses of the CITED2 peptide (0.68 ng, 3.4 ng, or 34 ng), the same amounts of a negative control peptide (CITED2 APAA) that is deficient in binding to the TAZ1 domain of CBP/p300 and competing with HIF-1α for CBP/p300 binding (*SI Appendix*, Fig. S2), or equivalent volumes of vehicle. Retinas from OIR mice injected with the CITED2 peptide had significantly decreased retinal NV and VO compared to both vehicle and CITED2 APAA peptide controls at P17 (Fig. 1 *A*–*C*). The expression of proangiogenic genes such as *Vegfa* and *Epo* and proinflammatory cytokines and chemokines such as *Il1b*, *Tnfa*, *Ccl2*, and *Ccl3* were significantly up-regulated in OIR retinas compared to normoxic retinas. These same genes were significantly down-regulated in OIR retinas after intravitreal injection of the CITED2 peptide (Fig. 1*D*), suggesting that the CITED2 peptide can regulate the hypoxic response and modulate activation of angiogenic molecules in the retina.

We hypothesized that the CITED2 peptide rescued NV and VO in the OIR model by inhibiting HIF-mediated transcription. To confirm the effect of the CITED2 peptide on HIF transcriptional activity, we performed a luciferase reporter assay using HEK293 cells transfected with a plasmid containing three copies of the hypoxia response element (HRE) upstream of the firefly luciferase gene. Luciferase activity was significantly reduced in CITED2 peptide-treated cells compared to CITED2 APAA peptide-treated cells (Fig. 1*E*). These data indicate that the CITED2 peptide inhibits the transcriptional activity of HIF in vitro and suggest that the reduction in NV and VO observed in the OIR experiments is due to HIF inhibition by the CITED2 peptide.

To further assess the mechanism underlying HIF inhibition by the CITED2 peptides in vivo, we generated Alexa488-conjugated peptides to identify cellular uptake and tissue localization of the CITED2 peptides. P12 OIR mice were injected with Alexa488-CITED2 peptide, Alexa488-CITED2 APAA peptide, or an equivalent volume of nonreactive Alexa488 dye, and retinas were harvested 12 h after intravitreal injection. The Alexa488-conjugated CITED2 peptides were widely distributed throughout the retina, whereas we did not observe fluorescence in retinas from eyes injected with Alexa488 dye alone (Fig. 2 *A* and *B*). Cryosections of Alexa488-CITED2 peptide-treated retinas show that the CITED2 peptide is taken up by cells in the inner plexiform layer (IPL), inner nuclear layer (INL), and outer plexiform layer (OPL), and that the CITED2 peptide localizes to the nuclei of cells in the INL (Fig. 2 *C* and *D*). In control experiments with the Alexa488-CITED APAA peptide (where we did not observe an inhibitory effect on NV, VO, or transcriptional activity), the peptide localized to the same regions (*SI Appendix*, Fig. S3).

To confirm which specific types of retinal cells are affected by the CITED2 peptide, we prepared a single cell suspension from OIR retinas and sorted for cells with Alexa488 fluorescence, indicating that they had taken up the Alexa488-labeled CITED2 peptides. This cell population was then probed for expression of representative retinal cell type-specific marker genes by RT-PCR. *Gfap*, *Vim*, *Glul*, and *Pax6* were highly expressed, indicating that the Alexa488-CITED2 peptide localized to astrocytes (*Gfap*), Muller glia (*Vim*/*Glul*), and ganglion cells and/or amacrine cells (*Pax6*). On the other hand, *Cd11b*, which is a marker for microglia, and *Tie2*, which is a marker for endothelial cells, were only weakly expressed in the cells that contained the Alexa488-CITED2 peptide, suggesting that the CITED2 peptide does not selectively localize to these cell types in OIR retinas (Fig. 2*E*). We then used RT-qPCR to assess the differences in gene expression in Alexa488-CITED2 peptide and Alexa488-CITED2 APAA peptide-containing cells. These data show that the expression of known HIF target genes such as *Vegfa*, *Epo*, *Ldha*, and *Ndufa4l2* were significantly down-regulated in CITED2 peptide-containing retinal cells compared to CITED2 APAA peptide-containing retinal cells (Fig. 2*F*), confirming that the CITED2 peptide specifically inhibits HIF transcriptional activity in the retina.

Given the striking effect of the CITED2 peptide in preventing pathological NV in the OIR model, we sought to characterize the general antiangiogenic potential of the CITED2 peptide. We performed an in vivo Matrigel plug assay, in which FGF2 and VEGF were used as proangiogenic factors to induce blood vessel formation and invasion of the Matrigel plug. Both FGF2 and VEGF induced formation of neovessels in Matrigel plugs 5 d after injection (Fig. 3*A*). When the CITED2 peptide was added to the Matrigel in combination with FGF2 prior to injection, FGF2-induced NV was visibly reduced (Fig. 3 *A* and *B*) and the percentage of CD45-negative/CD31-positive endothelial cells was also significantly decreased (Fig. 3 *A*–*D*). In contrast, the CITED2 peptide did not significantly reduce VEGF-induced NV in VEGF and CITED2 peptide containing Matrigel plugs (Fig. 3 *A*–*D*), suggesting that VEGF-driven vascular development in this assay is less dependent on HIF activation than FGF2-mediated angiogenesis.

We next observed whether the CITED2 peptides have effects on physiological retinal vascular development of normal mice. The mouse retinal vasculature develops during the first 21 d following birth. Vessels develop first in the superficial (inner) plexus from P0 to P8 using the astrocytes as a scaffold, then in the deep (outer) plexus from P7 to P12, and finally in the

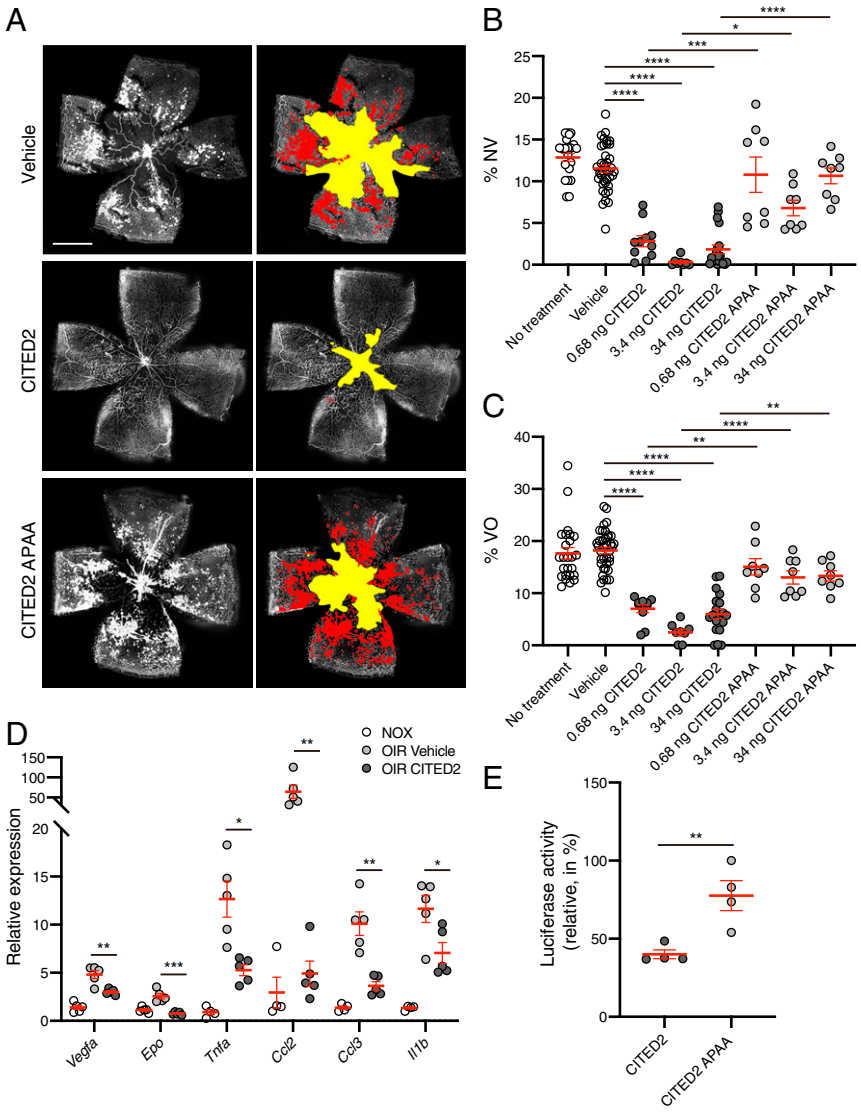

Fig. 1. The CITED2 peptide rescues retinal neovascularization and vaso-obliteration in OIR. (*A*) Immunofluorescent staining of P17 OIR retinas. OIR mice were intravitreally injected with vehicle (*Top*), the CITED2 peptide (0.68 ng) (*Middle*), or the CITED2 APAA peptide (0.68 ng) (*Bottom*). Retinal whole mounts were stained with GS-lectin. Representative images are shown on the *Left*; the same images are shown on the *Right* with NV highlighted in red and VO highlighted in yellow as used for quantification. (Scale bars, 1 mm.) (*B*) Quantification of the percentage of NV area in whole OIR retinas. (*C*) Quantification of the percentage of VO area in whole OIR retinas. For *B* and *C*, $n > 8$ per group. *P* values were calculated using one-way ANOVA with Tukey's multiple comparisons test. $^{*}P < 0.05$, $^{**}P < 0.01$, $^{***}P < 0.001$, $^{****}P < 0.0001$. The data represent at least three independent experiments. (*D*) Expression levels of proangiogenic genes (*Vegfa* and *Epo*) and proinflammatory genes (*Tnfa*, *Ccl2*, *Ccl3*, and *Il1b*) in P17 retinas. qPCR data are shown for total RNA isolated from the retinas of normoxic mice, vehicle-injected OIR mice, and CITED2 peptide-injected OIR mice ($n = 5$ per each group). *P* values were calculated using multiple *t* tests, $^{*}P < 0.05$, $^{**}P < 0.01$, $^{***}P < 0.001$. (*E*) Luciferase activity measured from HEK293 cells transfected with a luciferase reporter gene driven by a promoter containing three copies of the hypoxia response element and treated with the CITED2 peptide or the CITED2 APAA peptide ($n = 4$ per each group). *P* values were calculated using a two-tailed unpaired *t* test. $^{**}P < 0.01$. For *B*–*E*, the mean and SEM are shown in red.

intermediate plexus from P14 to P21 (24). To determine whether the CITED2 peptides have an effect on formation of the vasculature of the superficial plexus, we intravitreally injected the CITED2 peptide, CITED2 APAA peptide, and vehicle into normoxic C57/B6J mice on P2 and evaluated the formation of the superficial plexus at P6 (Fig. 4 *A*–*D*). The vascularized area and the number of branching points in the superficial plexus were slightly, but significantly, decreased in CITED2 peptide-injected eyes compared to CITED2 APAA peptide or vehicle-injected eyes. On the other hand, when we injected the CITED2 peptide into the eyes of P4 and P7 mice and analyzed retinal vasculature at P10 and P14, respectively, the number of vessel branching points of all layers were similar in CITED2 peptide- and vehicle-injected retinas (Fig. 4 *E*–*H*), suggesting that the CITED2 peptide has an effect on very early retinal vascular development of the superficial plexus but does not affect later stages of retinal vascular development.

Intravitreal injection of the anti-VEGF drugs aflibercept or ranibizumab is widely used to treat neovascular retinal diseases such as PDR and ROP as well as age-related macular degeneration (AMD), diabetic macular edema (DME), and RVO. However, as targeting VEGF is known to induce off-target effects (15), we investigated the ability of the CITED2 peptide to function synergistically with a lower dose of aflibercept in order to minimize the off-target effects of VEGF antagonists. While all doses (200 ng to 20 μg) of intravitreally injected aflibercept are capable

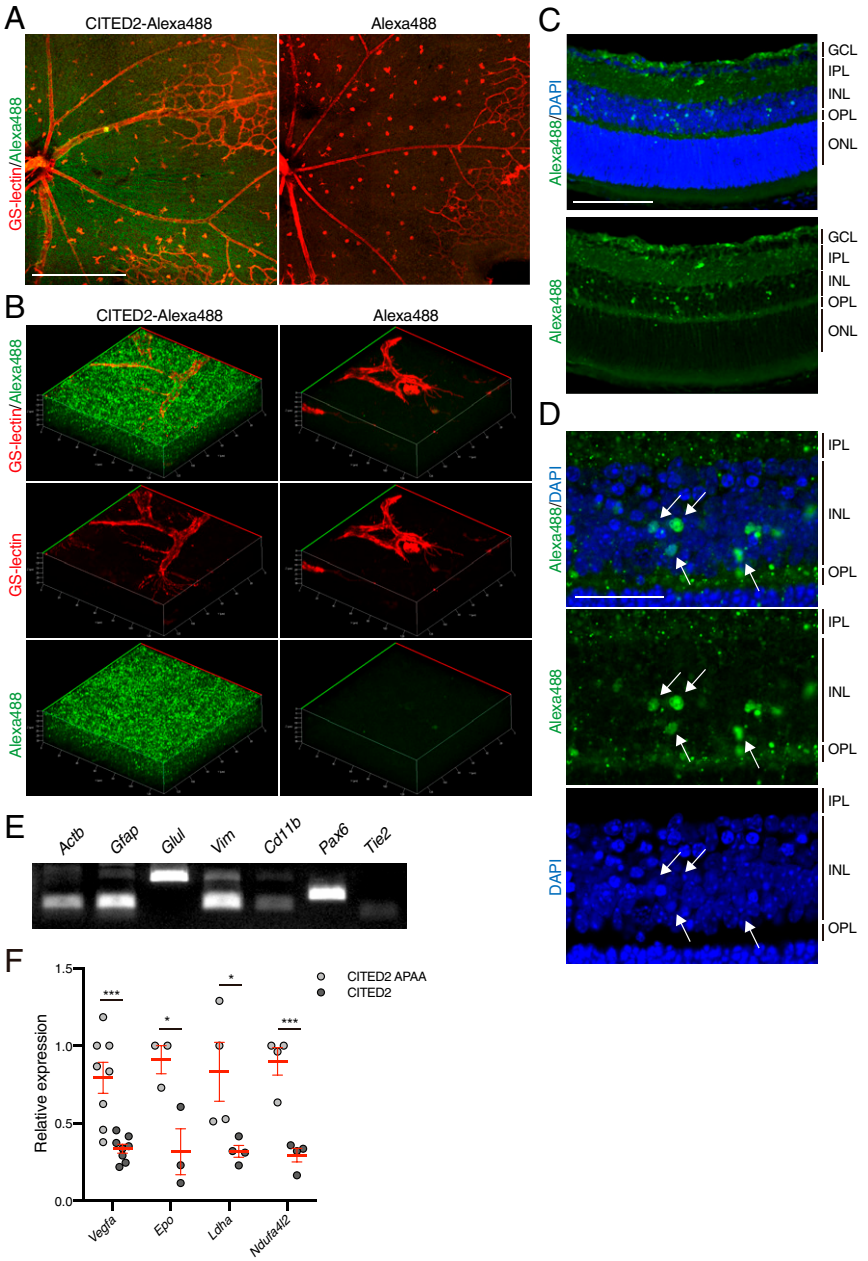

Fig. 2. The CITED2 peptide is widely distributed in various retinal cell types after intravitreal injection. (*A*) Alexa488-CITED2 peptide fluorescence can be observed in OIR retinas. A total of 2 μM of Alexa488-conjugated CITED2 peptide (*Left*) and nonreactive Alexa488 dye (*Right*) were intravitreally injected into OIR mice on P12. Retinas were harvested 12 h after injection and retinal whole mounts were stained with GS-lectin (red). (Scale bars, 500 μm.) (*B*) Three-dimensional images of retinal whole mounts shown in *A*. (*C*) Representative cryosection of an Alexa488-CITED2 peptide-injected OIR retina. Retinal tissue was harvested 12 h after intravitreal injection on P12 and stained with DAPI. (Scale bars, 100 μm.) GCL, ganglion cell layer; IPL, inner plexiform layer; INL, inner nuclear layer; OPL, outer plexiform layer; ONL, outer nuclear layer. (*D*) High magnification images of the inner nuclear layer shown in *C*. White arrows highlight nuclear localization of CITED2 peptides. (Scale bars, 50 μm.) (*E*) Expression of retinal cell type-specific markers in Alexa488-CITED2 peptide-injected OIR retinas. OIR retinas were harvested and digested into a single cell suspension 12 h after intravitreal injection of Alexa488-CITED2 peptide on P12. Alexa488-positive cells were sorted and the expression of retinal cell markers was confirmed by RT-PCR. *Actb*, β-actin; *Gfap*, glial fibrillary acidic protein; *Glul*, glutamine synthetase; *Vim*, vimentin. (*F*) Expression levels of known HIF target genes in CITED2 peptide-containing retinal cells and CITED2 APAA peptide-containing retinal cells after intravitreal injections ($n = 4$ per sample). *P* values were calculated using multiple *t* tests. $^*P < 0.05$, $^{***}P < 0.001$. The mean and SEM are shown in red.

of significantly reducing the area of NV in OIR retinas in a manner comparable to the CITED2 peptide, VO is not rescued with high doses of aflibercept (10 to 20 μg) that are comparable to the clinical dose in humans, and decreased VO is only observed for the lowest dose of aflibercept (200 ng) (Fig. 5*B* and *SI Appendix*, Fig. S4 *A–C*). However, in OIR eyes injected with a combination of 10 μg aflibercept and 3.4 ng of the CITED2 peptide, the area of VO was significantly smaller than observed for aflibercept monotherapy (Fig. 5*B*). With a lower 200-ng dose of aflibercept alone, the antineovascular effect is comparable to the higher dose of aflibercept (Fig. 5*C* and *SI Appendix*, Fig. S4 *A–C*). However, combination therapy of 200 ng of aflibercept and 3.4 ng of the CITED2 peptide significantly rescued both VO and NV (Fig. 5 *A–C*). Thus, combinations of the CITED2 peptide and

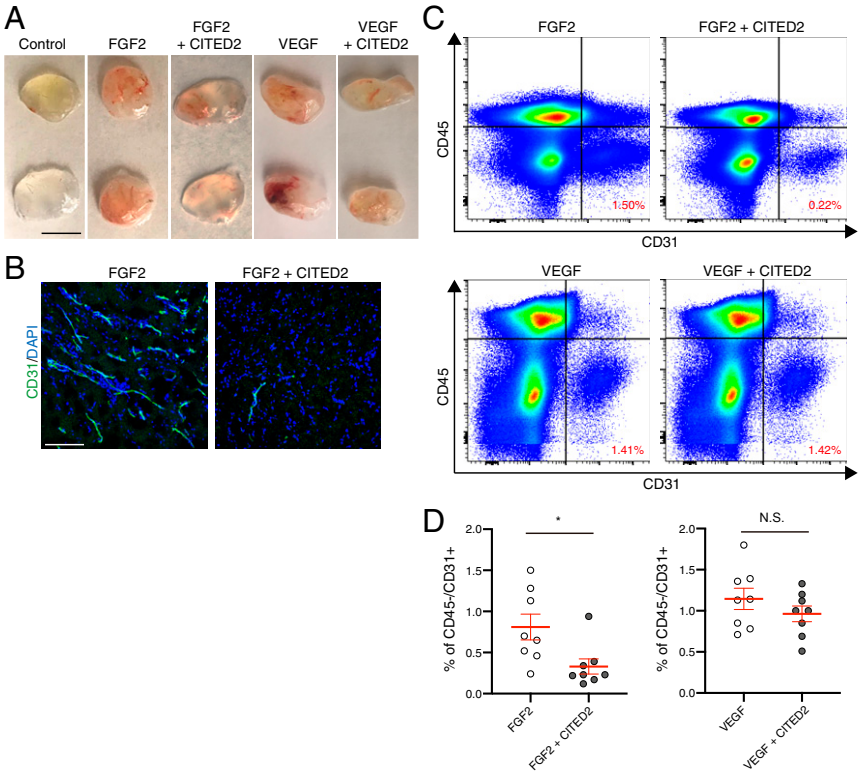

Fig. 3. The CITED2 peptide inhibits FGF2-induced neovascularization in the in vivo Matrigel plug assay. (*A*) Representative photos of Matrigel plugs that were removed from the s.c. space 5 d postinjection. (Scale bars, 1 cm.) (*B*) Cryosectioned Matrigel plugs were stained with the endothelial cell marker CD31 (green) and DAPI (blue). (Scale bars, 200 μm.) (*C*) Cell sorting from Matrigel plugs. Matrigel plugs were digested and stained with CD31 and CD45. The CD31 positive/CD45 negative fraction was considered to be endothelial cells. The percentage of cells in the CD31 positive/CD45 negative fraction is indicated in the *Lower Right* quadrant of the graphs in red. (*D*) Quantification of endothelial cells in Matrigel plugs ($n = 8$). *P* values were calculated using an unpaired two-tailed *t* test, $*P < 0.05$, N.S., not significant. The mean and SEM are shown in red.

aflibercept can promote revascularization of the avascular retina, an effect not observed for high-dose aflibercept treatment alone in OIR. Moreover, combined injection of aflibercept and the CITED2 peptide allows for a reduction in the dose of aflibercept, suggesting that the CITED2 peptide could be used in combination with anti-VEGF therapies to mitigate the off-target local and systemic effects of high doses of anti-VEGF drugs.

We then used RT-qPCR to assess the differences in gene expression in CITED2 peptide and aflibercept-treated OIR retinas. These data show that the expression levels of known HIF target genes such as *Vegfa*, *Epo*, *Ldha*, *Fgf11*, and *Ndufa4l2* were significantly down-regulated in CITED2 peptide-treated OIR retinas compared to aflibercept-treated retinas (Fig. 5*D*), confirming that the CITED2 peptide functions as a negative regulator of HIF transcriptional activity, whereas aflibercept functions by targeting circulating VEGF and thus does not have a similar suppressive effect on transcription of HIF target genes. We additionally observe that the amount of VEGF in P15 OIR retinas is higher for aflibercept-treated retinas than for CITED2 peptide-treated retinas (Fig. 5*E*), suggesting that directly targeting the circulating pool of VEGF results in compensatory up-regulation of angiogenic cytokines, a phenomenon that has previously been observed in both the mouse and rat OIR models (25, 26). Taken together, these data highlight the potential therapeutic benefit of combining anti-VEGF therapies like aflibercept and the CITED2 peptide, an inhibitor of HIF-driven transcription, for treatment of pathological NV in patients with ischemic retinal diseases.

Discussion

We have demonstrated that a peptide derived from the intrinsically disordered protein CITED2, a potent negative feedback regulator of HIF-1α, can significantly rescue hypoxia-induced NV and VO in the OIR model of ischemic retinopathy. Intravitreal injection of the CITED2 peptide results in down-regulation of HIF-mediated transcription in retinal cells that play critical roles in driving both developmental and pathological angiogenesis. Interestingly, the CITED2 peptide not only suppresses pathological NV in the OIR model but it also facilitates revascularization of the ischemic retina. This is in contrast to anti-VEGF agents, which suppress retinal vaso-permeability and proliferation, but not VO, in the OIR model. The beneficial effects of the CITED2 peptide on both NV and VO can be preserved in combination with reduced doses of the anti-VEGF drug aflibercept. Our studies suggest that direct inhibition of HIF-mediated transcription in the retina by the CITED2 peptide, alone or in combination with VEGF-targeting molecules, may have advantages over current therapeutic strategies for targeting retinal neovascularization.

During the hypoxic phase of OIR (P12 to P17), increased expression of proangiogenic HIF target genes leads to pathological NV (27). In OIR, the protein levels of HIF-1α and HIF-2α are known to be rapidly up-regulated after mice are returned to room air from hyperoxia on P12 (27). As *Cited2* is a known HIF target gene, we also confirmed that expression of *Cited2* in the retina is up-regulated early in the hypoxic phase of OIR (*SI Appendix*, Fig. S5). However, the amounts of NV and VO observed in untreated or vehicle-injected OIR retinas suggest that the endogenous amounts of CITED2 are not sufficient to rescue hypoxia-driven angiogenesis in the OIR retina. Intravitreal injection of the CITED2 peptide on P12 down-regulates HIF-mediated transcription (Figs. 1*E* and 2*F*), suggesting that the exogenous peptide is able to complement the effects of the endogenously expressed CITED2, leading to more robust

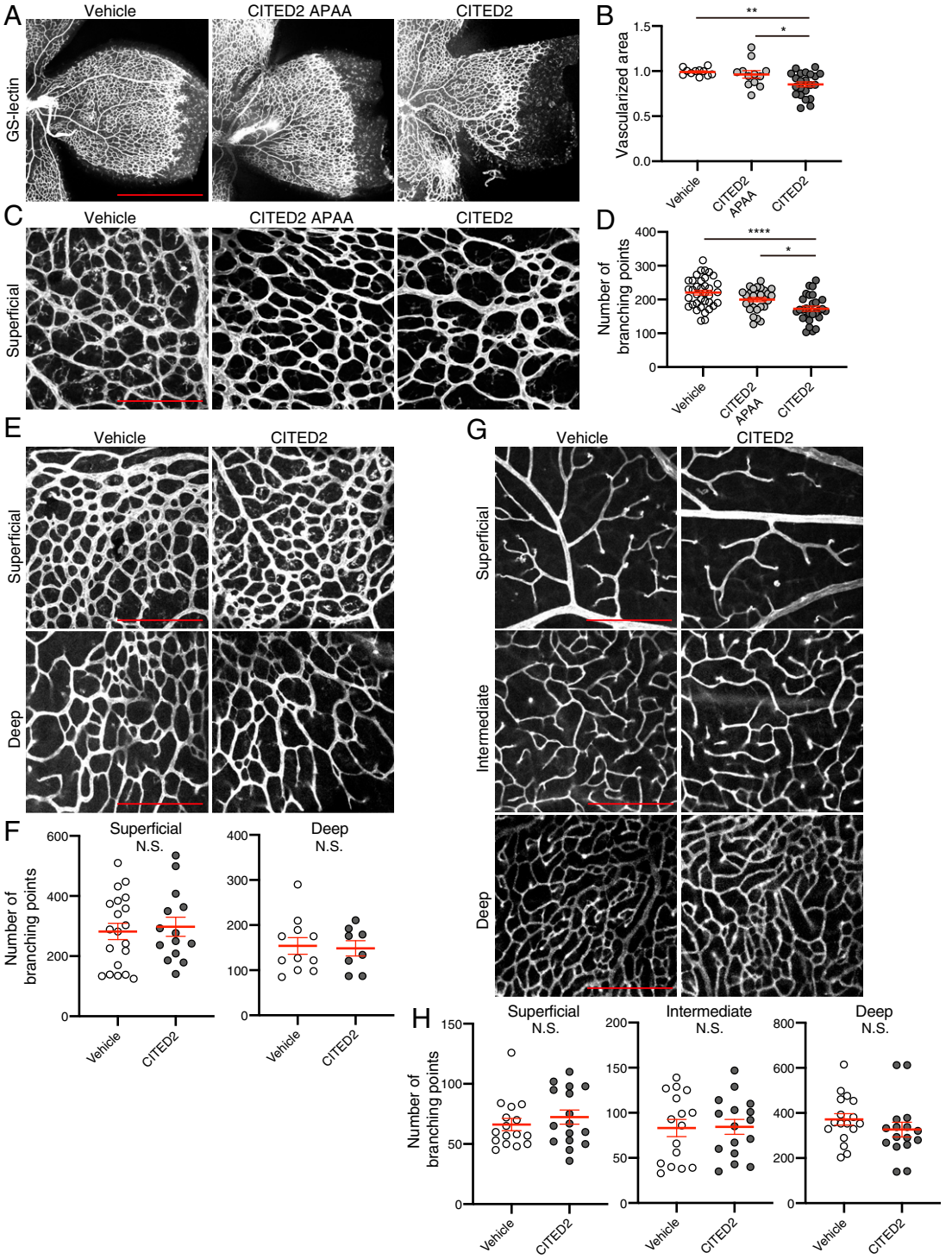

Fig. 4. The CITED2 peptide delays early development of retinal vasculature, but does not affect later stages of vascular development. (*A*) Representative images of retinal vasculature in CITED2 peptide-treated retinas and control retinas on P6. Normoxic mice were intravitreally injected with CITED2 peptide (34 ng), CITED2 APAA peptide (34 ng), or vehicle on P2 and retinas were harvested on P6 and stained with GS-lectin. (Scale bars, 1 mm.) (*B*) Quantification of the percentage of vascularized area in P6 retinas. *P* values were calculated using one-way ANOVA and Tukey's multiple comparisons test ($n > 8$ per each group). $*P < 0.05$, $**P < 0.01$. (*C*) High magnification images of the images shown in *A*. (Scale bars, 200 μm.) (*D*) Branching points were counted from the images shown in *C*. *P* values were calculated using one-way ANOVA and Tukey's multiple comparisons test ($n > 8$ per each group). $*P < 0.05$, $****P < 0.0001$. (*E*) Normoxic mice were intravitreally injected with the CITED2 peptide (34 ng) or vehicle on P4 and retinas were harvested at P10 and stained with GS-lectin. Representative images from the superficial plexus (*Top*) and deep plexus (*Bottom*) are shown. (Scale bars, 200 μm.) (*F*) The number of branching points in each layer of the P10 retinas was quantified and *P* values were calculated using an unpaired two-tailed *t* test ($n > 8$ per each group). N.S., not significant. (*G*) Normoxic mice were intravitreally injected with the CITED2 peptide (34 ng) or vehicle on P7 and retinas were harvested at P14 and stained with GS-lectin. Representative images from the superficial plexus, intermediate plexus, and deep plexus are shown. (Scale bars, 200 μm.) (*H*) The number of branching points in each layer of the P14 retinas was quantified and *P* values were calculated using an unpaired two-tailed *t* test ($n > 8$ per each group). N.S., not significant. For *B*, *D*, *F*, and *H*, the mean and SEM are shown in red.

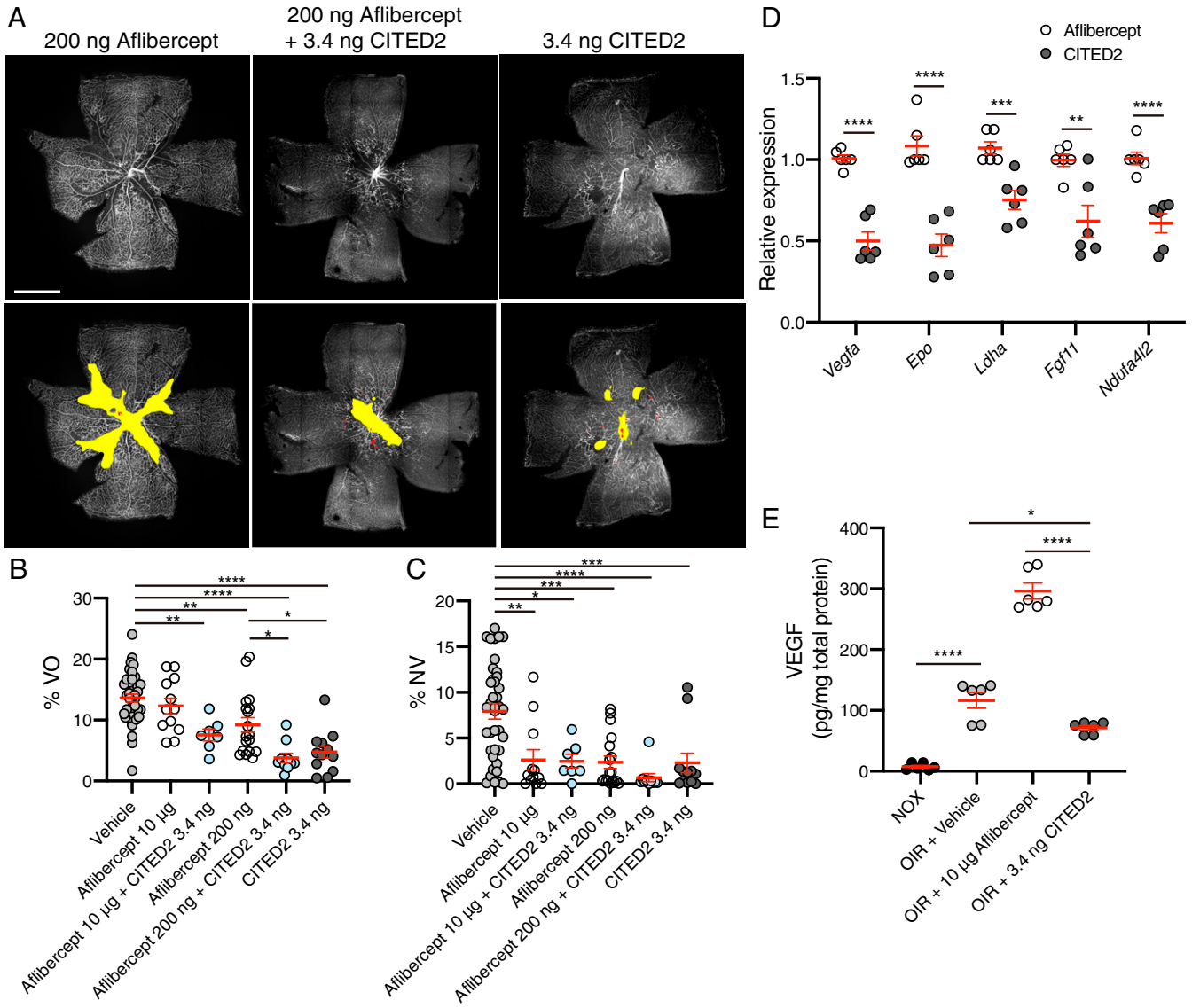

Fig. 5. Combination therapy of the CITED2 peptide and aflibercept rescues retinal neovascularization and vaso-obliteration in OIR. (*A*) Immunofluorescent staining of OIR retinas at P17 after intravitreal injection of aflibercept (200 ng), aflibercept and CITED2 peptide (200 ng aflibercept and 3.4 ng CITED2 peptide), or CITED2 peptide (3.4 ng) at P12. Retinal whole mounts were stained with GS-lectin. Representative images for each treatment are shown (*Upper*) and the same images are shown (*Lower*) with NV highlighted in red and VO highlighted in yellow as used for quantification. (Scale bars, 1 mm.) (*B*) Quantification of the percentage of VO area in whole retinas. (*C*) Quantification of the percentage of NV area in whole retinas. For *B* and *C*, $n > 7$ per group. *P* values were calculated using one-way ANOVA with Tukey's multiple comparisons test. $*P < 0.05$, $**P < 0.01$, $***P < 0.001$, $****P < 0.0001$. (*D*) Validation of expression of HIF target genes in CITED2- and aflibercept-treated OIR retinas. Total RNA was isolated 24 h after intravitreal injection of CITED2 peptide (3.4 ng) or aflibercept (10 µg) on P12 ($n = 6$ per group). *P* values were calculated using multiple *t* tests. $**P < 0.01$, $***P < 0.001$, $****P < 0.0001$. (*E*) Quantification of VEGF protein levels in P15 retinas by ELISA ($n = 6$ per group). *P* values were calculated using one-way ANOVA with Tukey's multiple comparisons test. $*P < 0.05$, $****P < 0.0001$. For *B*–*E*, the mean and SEM are shown in red.

suppression of HIF transcriptional activation. Our data indicate that supplementing the available amount of an endogenous negative feedback regulator of HIF-mediated transcription can be of benefit for reducing pathological NV and vaso-obliteration in OIR.

Our prior in vitro studies of the CITED2 peptide showed that CITED2 functions as an allosteric inhibitor of HIF-1α by competing for a partially overlapping binding site on the TAZ1 domain of the transcriptional coactivators CBP/p300 (20). CITED2 efficiently displaces the intrinsically disordered C-terminal domain of HIF-1α from TAZ1 but the reverse process, displacement of CITED2 by HIF-1α, is highly unfavorable, leading us to postulate that CITED2 and TAZ1 function as a hypersensitive, unidirectional switch to terminate the hypoxic response (20). The ability of the CITED2 peptide to rescue NV and VO in the OIR model (but not the CITED2 APAA peptide, which lacks a key binding motif required for effective competition with HIF-1α), suggests that it functions by a similar mechanism to compete with HIF in vitro and in vivo. The CITED2 peptide is highly potent, even when delivered to the vitreous at low nanomolar concentrations. Alexa488-labeled CITED2 peptides injected intravitreally into OIR eyes are taken up by retinal cells and localize in Muller glia, astrocytes, Pax6-positive retinal neurons, ganglion cells, and amacrine cells (Fig. 2). Transcript levels of known HIF target genes are down-regulated in Alexa488-CITED2 peptide-containing cell populations relative to the transcript levels from

cells that had taken up the Alexa488-CITED2 APAA control peptide (Fig. 2*F*). Stabilization of HIF in OIR retinas is known to mainly occur in Muller glia, astrocytes, ganglion cells, and neurons in the inner nuclear layer of the avascular zone (27) and recent work by Nathans and colleagues confirmed the critical and distinct roles of HIF-1α and HIF-2α in retinal neurons and Muller glia, respectively, in the development of retinal vasculature (28). The distinct tissue localization pattern observed for the CITED2 peptides suggests that the effect on NV and VO in OIR retinas injected with the CITED2 peptide is due to specific inhibition of HIF transcriptional activity in retinal cell types that are known to express HIF-1α and HIF-2α. While our prior biophysical studies focused on the ability of CITED2 to compete with HIF-1α, we expect that the CITED2 peptide has similar inhibitory effects on HIF-1α and HIF-2α in vivo. The C-terminal disordered domain of HIF-1α and HIF-2α is highly conserved, and it has been demonstrated that CITED2 can inhibit both HIF-1α and HIF-2α in vitro (29). Thus, the present experiments strongly support our postulated model of a CITED2-driven regulatory switch (20) that attenuates HIF-mediated transcription and underscore the central role of intrinsically disordered proteins in regulation of cellular signaling (30).

The ability of the CITED2 peptide to function as an inhibitor of HIF-mediated transcription is further confirmed by the results of the in vivo Matrigel plug assay. While we did not observe a significant reduction in VEGF-induced NV in Matrigel plugs containing the CITED2 peptide, we did observe a significant reduction in FGF2-induced NV and endothelial cell migration in CITED2 peptide-containing Matrigel plugs (Fig. 3). Although *Vegfa* transcription is under the control of HIF in hypoxic tissues, the high concentration of VEGF already present in the Matrigel plug likely minimizes the ability to observe a physiological effect due to reduction in expression of *Vegfa* and other proangiogenic cytokines as a consequence of HIF inhibition by the CITED2 peptide—even large changes in HIF transcriptional activity would be unlikely to counteract the high concentrations of VEGF present in the Matrigel plug. On the other hand, FGF2 is known to function as part of a positive feedback loop for HIF activation to drive angiogenesis in endothelial cells (31). It is likely that the CITED2 peptide is able to potently disrupt this positive feedback loop by negatively regulating HIF transcriptional activation, resulting in suppression of NV in FGF2-containing Matrigel plugs.

In our current study, intravitreal injection of the CITED2 peptide on P2 delays vascular development in the superficial plexus; however, development of the deep plexus and intermediate plexus vasculature was not affected by CITED2 peptide injection at P4 or P7, respectively (Fig. 4). These data suggest that intravitreal injection of the CITED2 peptide does not influence physiological retinal vascular development except during the very early developmental stage. CITED2 has been shown to play an important role in vascular development in the mouse eye. Loss of CITED2 is embryonic lethal, thus precluding the analysis of effects on the retinal vasculature, which develops after birth. However, aberrant hyaloid vasculature is observed at the embryonic stage in CITED2 knockout mice, resulting from dysregulation of HIF-1α and VEGF (32, 33). Taken together, these results further support the ability of CITED2 to regulate HIF-mediated angiogenesis and modulate the availability of proangiogenic cytokines like VEGF.

Aflibercept is widely known to inhibit retinal NV by blocking VEGF, but at doses comparable to those used in the clinic it does not result in diminished VO in OIR retinas. In fact, aflibercept has been observed to exacerbate VO in a dose-dependent manner, suggesting that targeting VEGF may also block revascularization of the avascular zone in OIR (Fig. 5 *A* and *B* and *SI Appendix*, Fig. S4) (34). Previous studies from our laboratory demonstrated that angiogenic and trophic factors secreted by astrocytes, including VEGF, are required for revascularization of the avascular zone in the OIR model (35), suggesting that targeting factors upstream of VEGF and other drivers of angiogenesis would be beneficial. The CITED2 peptide functions by inhibiting HIF transcriptional activity and modulating the availability of key angiogenic factors such as VEGF, rather than by directly targeting the proangiogenic cytokines already present in the retina. Consistent with our experiments with the CITED2 peptide alone (Fig. 1), OIR mice injected with both the CITED2 peptide and aflibercept demonstrate significant revascularization of the avascular region, even though equivalent doses of aflibercept alone did not promote revascularization to a similar extent (Fig. 5 and *SI Appendix*, Fig. S4). Notably, beneficial effects on both NV and VO were observed in OIR retinas treated with a combination of the CITED2 peptide and aflibercept, even when the concentration of aflibercept was reduced by 50-fold. These results highlight that dual targeting of the HIF transcription factors and VEGF may be advantageous for the treatment of ischemic retinal diseases, as treatment with the CITED2 peptide allows for potent inhibition of pathological NV without interfering with repair processes that promote revascularization of the avascular zone in OIR retinas or impairing nondevelopmental angiogenesis (Fig. 4). Revascularization of OIR retinas treated with the CITED2 peptide or combinations of the CITED2 peptide and aflibercept likely results from the ability to fine tune the amount of VEGF and other proangiogenic factors available for restoring retinal vasculature, without allowing these critical cytokines to accumulate to levels that would promote pathological neovascularization.

Clinical observations suggest that the adverse effects of anti-VEGF drugs on worsening of macular ischemia in the long term should be considered, particularly in eyes with significant ischemia at baseline and after repeated intraocular anti-VEGF injections (36). Intravitreal injection of anti-VEGF drugs can suppress plasma VEGF levels below the detectable limit within 3 h after injection and this suppressive effect can last more than 7 d in patients with AMD, DME, and RVO and for up to 12 wk after injection in patients with ROP (37, 38). However, VEGF plays critical roles in a number of physiological processes and thus sustained systemic reduction of VEGF may lead to complications (15, 39–46). Because of the potential off-target effects of VEGF antagonists, combination therapies that reduce the dose of VEGF antagonists, like the combination of aflibercept and the CITED2 peptide used here, may provide a lower risk alternative for treating high-risk patients.

Much effort has been directed toward pharmacological targeting of the HIF transcription factors over the past two decades, and a large number of therapeutic compounds have been developed with the goal of specifically modulating HIF stability and transcriptional activity for various applications, including cancer, cardiovascular disease, and ocular vascular diseases (47–50). Our findings suggest that targeting HIF transcriptional activation in the ischemic retina through administration of a peptide derived from CITED2, a negative regulator of HIF-mediated transcription, is beneficial for inhibiting pathological neovascularization as well as promoting the normalization of disrupted vasculature in the ischemic retina. These studies highlight the potential utility of targeting the HIF transcription factors for treatment of neovascular retinal diseases, a leading cause of blindness in developed countries, and suggest that peptide-based inhibitors may present new opportunities for intervention in the many diseases that are exacerbated by prolonged or intermittent hypoxia.

Materials and Methods

Reagents. Peptides of the CITED2 C-terminal transactivation domain (residues 216 to 269 of human/mouse CITED2 with the pentapeptide sequence GSHMS at the N terminus) were expressed in *Escherichia coli* and purified as described previously (20). The L243A/E245A/L246A mutations for the CITED2

APAA mutant peptide were introduced using standard site-directed mutagenesis protocols. The peptides were stored as lyophilized powders and resuspended and dialyzed into buffer containing 20 mM Tris pH 6.8, 50 mM NaCl, and 2 mM dithiothreitol (DTT) prior to use. The identity and purity of all peptides was confirmed by mass spectrometry.

The CITED2 peptides contain a single cysteine residue (C261) and were fluorescently labeled with a three- to fivefold excess of AlexaFluor 488 C_5 maleimide dye (Invitrogen) in 50 mM Tris pH 7.2. Unreacted dye was removed during buffer exchange into 20 mM Tris pH 6.8, 50 mM NaCl, and 2 mM DTT on a NAP-5 column (GE). For fluorescent dye controls, nonreactive AlexaFluor 488 dye was prepared by dissolving AlexaFluor 488 carboxylic acid, tetrafluorophenyl (TFP) ester (Invitrogen) in water adjusted to pH 9.0 with sodium hydroxide and incubating overnight to hydrolyze the ester and eliminate amine reactivity.

Aflibercept (Eylea; Regeneron Pharmaceutical) was diluted in 20 mM Tris pH 6.8, 50 mM NaCl, and 2 mM DTT. One microgram (0.5 μL) of normal human IgG (R&D Systems 1-001-A) was used as a control.

Fluorescence Anisotropy Competition Experiments. Fluorescence anisotropy competition assays were carried out in 20 mM Tris pH 6.8, 50 mM NaCl, and 2 mM DTT on a Horiba Fluorolog-3 fluorimeter at 25 °C. Alexa 594-labeled HIF-1α and CITED2 peptides were prepared as previously described (20). For competition assays, unlabeled CITED2 peptides were titrated into a preformed complex of 20 nM Alexa594-HIF-1α and 250 nM TAZ1 or 20 nM Alexa594-CITED2 and 250 nM TAZ1. Data were analyzed as described previously (20) using GraphPad Prism 8 (GraphPad Software, Inc.).

Animal Experiments. C57BL/6J mice were obtained from the animal facility at The Scripps Research Institute. OIR was induced as previously described (23). Briefly, C57BL/6J mouse pups and their mother were exposed to 75% oxygen from P7 to P12 and subsequently transferred to room air. Retinal NV and VO were analyzed at P17.

Quantification of OIR. The percentage of the area of NV and VO in OIR retinas was automatically quantified using deep learning segmentation software available at oirseg.org (51).

Intravitreal Injections. P12 C57BL/6J OIR pups and P2, P4, and P7 normoxic mice were injected in the vitreous cavity with 0.5 μL of CITED2 peptide, CITED2 APAA peptide, aflibercept or vehicle control using a 10-μL Hamilton syringe with a 34-gauge needle.

Luciferase Assay. HEK293 cells were transfected using Lipofectamine 2000 (Invitrogen) with 0.5 μg of pGL2-HRE (Addgene 26731) and were cotransfected with 0.63 μg of CITED2 peptide or 0.63 μg CITED2 APAA mutant peptide according to the manufacturer's protocol. After 24-h incubation, cells were washed with phosphate buffered saline (PBS) and lysed with the luciferase cell culture lysis reagent (Promega), and the luciferase assay was performed using the luciferase assay system (Promega E1500) according to the manufacturer's protocol.

Sorting for Mouse Retinal Cells. A total of 2 μM of Alexa488-conjugated CITED2 or CITED2 APAA peptides were injected into both eyes of P12 OIR mice. Retinas were collected 16 h after injection and transferred into cold PBS with Ca^{2+}/Mg^{2+}. A postnatal neural dissociation kit (Miltenyi, 130-092-628) was used to prepare a single cell suspension from mouse retinas. The resuspended cells [in 500 μL of PBS with 1% fetal bovine serum (FBS)] were stained with DAPI (1:1,000) for exclusion of dead cells. The cells were sorted and analyzed using a FACS Aria flow cytometer (BD) with FlowJo (BD) software. Alexa488 positive and negative cells were sorted from the live cell population. Total RNA was isolated from sorted cells using the RNeasy Micro Kit (Qiagen) and reverse transcribed using Maxima First Strand cDNA Synthesis Kit for RT-qPCR (Thermo Scientific). For retinal cell profiling, PCR was performed using PrimeSTAR GXL DNA polymerase on a T100 Thermal Cycler (Bio-Rad) and the cycling program was 25 cycles of 94 °C for 30 s, 58 °C for 30 s, and 72 °C for 30 s. qPCR was performed using Power SYBR Green PCR Master Mix (Thermo Fisher Scientific) on a Quantstudio 5 Real-Time PCR System (Thermo Fisher Scientific) and *36b4* was used as the reference gene. Primer sequences are listed in *SI Appendix*, Table S1.

Retinal Immunofluorescence. Retinas were dissected and prepared for whole mounts or sectioning. For retinal whole mounts, dissected retinas were placed in 4% paraformaldehyde (PFA) for 1 h. After fixation, the vitreous was removed and the retinas were laid flat with four radial relaxing incisions and incubated overnight with Alexa568-conjugated isolectin Griffonia simplicifolia IB-4 (GS-lectin) (Thermo Fisher Scientific, I21413). Retinas were washed in PBS and mounted with ProLong Diamond Antifade mounting medium (Thermo Fisher Scientific, P36965). For preparation of cross-sections, dissected eyes were incubated in 4% PFA for 3 h. Retinas were then placed in 20% sucrose at 4 °C for 3 h and embedded in Tissue-Tek optimal cutting temperature (OCT) compound (Sakura Finetek) for cryosectioning. The 12-μm retinal sections were washed in PBS and incubated with DAPI to visualize cell nuclei. Images were obtained using a confocal microscope (LSM710, Carl Zeiss).

Real-Time PCR Analysis. For qPCR, single retinas were collected in 500 μL of TRIzol and total RNA was isolated using a PureLink RNA Mini Kit (Thermo Fisher Scientific) according to manufacturer's instructions. A total of 750 ng of RNA was used for RT-qPCR using a high-capacity cDNA reverse transcription kit (Thermo Fisher Scientific). qPCR was performed using Taqman universal master mix (Thermo Fisher Scientific) and Taqman probes or Power SYBR Green PCR Master Mix (Thermo Fisher Scientific) and primers on a Quantstudio 5 Real-Time PCR System (Thermo Fisher Scientific). β-Actin (*Actb*) was used as the reference gene for all experiments. Primer sequences and Taqman assays are listed in *SI Appendix*, Tables S1 and S2, respectively.

In Vivo Matrigel Plug Assay. Matrigel Growth Factor Reduced Basement Membrane Matrix, lactose dehydrogenase elevating virus (LDEV)-free (Corning) was mixed with 1,000 ng/mL recombinant VEGF165 (PeproTech 100-20) or 500 ng/mL of FGF2 (PeproTech 450-33) and 1 μM CITED2 peptide or control vehicle on ice. A total of 500 μL of Matrigel was injected s.c. on both flanks on the abdominal side after shaving under anesthesia (100 mg/kg ketamine and 10 mg/kg xylazine). After 5 d, mice were killed and Matrigel plugs removed, photographed, fixed with 4% PFA, and embedded in OCT. To visualize endothelial cells that migrated into the Matrigel plug, cryosectioned plugs were stained with CD31 antibody (BD 550274) and DAPI.

FACS analysis was used to quantify the neovessels in the plugs as previously described (52). The Matrigel plugs were digested by incubating for 1 h at 37 °C with an enzymatic mixture containing 25 μg/mL of hyaluronidase (MP Biomedical), 25 μg/mL of DNase (Sigma-Aldrich), 3 U/mL of dispase (Roche), and 3 U/mL of liberase (Roche) dissolved in PBS. The suspension was washed, filtered, and stained with CD31-FITC (Biolegend 102405) and CD45-Bv421 (Biolegend 103133). Samples were analyzed with a FACS LSR II flow cytometer (Becton Dickinson Immunocytometry Systems) and data analysis was performed in FlowJo v10 (BD). Endothelial cells were present in the CD31-positive and CD45-negative populations.

ELISAs. Retinal tissue was homogenized in 250 μL of PBS and stored overnight at ≤ −20 °C. After two freeze–thaw cycles, the homogenates were centrifuged for 5 min at 5,000 × *g*. Total protein was quantified using a bicinchoninic acid (BCA) assay according to the manufacturer's protocol (Pierce). Supernatants were then assayed without dilution in duplicate using the Mouse VEGF Quantikine ELISA kit (R&D Systems) according to the manufacturer's protocol.

Statistical Analysis. All statistical tests were performed in GraphPad Prism 8 (GraphPad Software, Inc). Data comparisons between two groups were performed using unpaired two-tailed Student's *t* tests or multiple *t* tests. Data comparisons between multiple groups were performed with one-way ANOVA with Tukey's correction. Statistical tests used for each experiment are specified in the figure legends. Data are represented as mean ± SEM unless otherwise indicated. A P value <0.05 was considered significant.

Study Approval. All animal protocols were approved by the institutional animal care and use committee at The Scripps Research Institute, La Jolla, CA and we adhered to all federal animal experimentation guidelines.

Data Availability. All study data are included in the article and supporting information.

ACKNOWLEDGMENTS. We thank the members of the M.F. and P.E.W. laboratories, our colleagues at the Lowy Medical Research Institute, and Prof. Jane Dyson for many helpful discussions regarding the direction of this project and the data presented in this manuscript. This work was supported by the Lowy Medical Research Institute (M.F.), the Skaggs Institute for Chemical Biology (P.E.W.), and NIH grants EY11254 (to M.F.) and CA096865 and CA229652 (to P.E.W.). R.B.B. was partially supported by a postdoctoral fellowship from the American Cancer Society (125343-PF-13-202-01-DMC). A.U.-O. is supported by a fellowship from the Manpei Suzuki Diabetes Foundation and Japan Society for the Promotion of Science (JSPS) KAKENHI Grant 17K16984.

1. N. D. Wangsa-Wirawan, R. A. Linsenmeier, Retinal oxygen: Fundamental and clinical aspects. *Arch. Ophthalmol.* **121**, 547–557 (2003).
2. R. A. Linsenmeier, H. F. Zhang, Retinal oxygen: From animals to humans. *Prog. Retin. Eye Res.* **58**, 115–151 (2017).
3. Y. Usui *et al*., Angiogenesis and eye disease. *Annu. Rev. Vis. Sci.* **1**, 155–184 (2015).
4. M. Friedlander, Fibrosis and diseases of the eye. *J. Clin. Invest.* **117**, 576–586 (2007).
5. S. V. Reddy, D. Husain, Panretinal photocoagulation: A review of complications. *Semin. Ophthalmol.* **33**, 83–88 (2018).
6. Anonymous; The Diabetic Retinopathy Study Research Group, Preliminary report on effects of photocoagulation therapy. *Am. J. Ophthalmol.* **81**, 383–396 (1976).
7. L. P. Aiello *et al*., Suppression of retinal neovascularization in vivo by inhibition of vascular endothelial growth factor (VEGF) using soluble VEGF-receptor chimeric proteins. *Proc. Natl. Acad. Sci. U.S.A.* **92**, 10457–10461 (1995).
8. N. Ferrara, R. S. Kerbel, Angiogenesis as a therapeutic target. *Nature* **438**, 967–974 (2005).
9. A. N. Witmer, G. F. Vrensen, C. J. Van Noorden, R. O. Schlingemann, Vascular endothelial growth factors and angiogenesis in eye disease. *Prog. Retin. Eye Res.* **22**, 1–29 (2003).
10. Y. Zhao, R. P. Singh, The role of anti-vascular endothelial growth factor (anti-VEGF) in the management of proliferative diabetic retinopathy. *Drugs Context* **7**, 212532 (2018).
11. A. L. Wu, W. C. Wu, Anti-VEGF for ROP and pediatric retinal diseases. *Asia Pac. J. Ophthalmol. (Phila.)* **7**, 145–151 (2018).
12. J. G. Gross *et al*.; Writing Committee for the Diabetic Retinopathy Clinical Research Network, Panretinal photocoagulation vs intravitreous ranibizumab for proliferative diabetic retinopathy: A randomized clinical trial. *JAMA* **314**, 2137–2146 (2015).
13. M. S. Ip, A. Domalpally, J. K. Sun, J. S. Ehrlich, Long-term effects of therapy with ranibizumab on diabetic retinopathy severity and baseline risk factors for worsening retinopathy. *Ophthalmology* **122**, 367–374 (2015).
14. M. Ashraf, A. A. Souka, R. P. Singh, Central retinal vein occlusion: Modifying current treatment protocols. *Eye (Lond.)* **30**, 505–514 (2016).
15. A. Usui-Ouchi, M. Friedlander, Anti-VEGF therapy: Higher potency and long-lasting antagonism are not necessarily better. *J. Clin. Invest.* **129**, 3032–3034 (2019).
16. R. K. Vadlapatla, A. D. Vadlapudi, A. K. Mitra, Hypoxia-inducible factor-1 (HIF-1): A potential target for intervention in ocular neovascular diseases. *Curr. Drug Targets* **14**, 919–935 (2013).
17. G. L. Semenza, HIF-1 and human disease: One highly involved factor. *Genes Dev.* **14**, 1983–1991 (2000).
18. G. L. Semenza, Hypoxia-inducible factor 1: Oxygen homeostasis and disease pathophysiology. *Trends Mol. Med.* **7**, 345–350 (2001).
19. S. Bhattacharya *et al*., Functional role of p35srj, a novel p300/CBP binding protein, during transactivation by HIF-1. *Genes Dev.* **13**, 64–75 (1999).
20. R. B. Berlow, H. J. Dyson, P. E. Wright, Hypersensitive termination of the hypoxic response by a disordered protein switch. *Nature* **543**, 447–451 (2017).
21. Z. Arany *et al*., An essential role for p300/CBP in the cellular response to hypoxia. *Proc. Natl. Acad. Sci. U.S.A.* **93**, 12969–12973 (1996).
22. D. Lando, D. J. Peet, D. A. Whelan, J. J. Gorman, M. L. Whitelaw, Asparagine hydroxylation of the HIF transactivation domain a hypoxic switch. *Science* **295**, 858–861 (2002).
23. L. E. Smith *et al*., Oxygen-induced retinopathy in the mouse. *Invest. Ophthalmol. Vis. Sci.* **35**, 101–111 (1994).
24. P. Sapieha, Eyeing central neurons in vascular growth and reparative angiogenesis. *Blood* **120**, 2182–2194 (2012).
25. M. McCloskey *et al*., Anti-VEGF antibody leads to later atypical intravitreous neovascularization and activation of angiogenic pathways in a rat model of retinopathy of prematurity. *Invest. Ophthalmol. Vis. Sci.* **54**, 2020–2026 (2013).
26. M. I. Dorrell, E. Aguilar, L. Scheppke, F. H. Barnett, M. Friedlander, Combination angiostatic therapy completely inhibits ocular and tumor angiogenesis. *Proc. Natl. Acad. Sci. U.S.A.* **104**, 967–972 (2007).
27. F. M. Mowat *et al*., HIF-1α and HIF-2α are differentially activated in distinct cell populations in retinal ischaemia. *PLoS One* **5**, e11103 (2010).
28. A. Rattner, J. Williams, J. Nathans, Roles of HIFs and VEGF in angiogenesis in the retina and brain. *J. Clin. Invest.* **129**, 3807–3820 (2019).
29. C. J. Hu *et al*., Differential regulation of the transcriptional activities of hypoxia-inducible factor 1α (HIF-1α) and HIF-2α in stem cells. *Mol. Cell. Biol.* **26**, 3514–3526 (2006).
30. P. E. Wright, H. J. Dyson, Intrinsically disordered proteins in cellular signalling and regulation. *Nat. Rev. Mol. Cell Biol.* **16**, 18–29 (2015).
31. M. Calvani, A. Rapisarda, B. Uranchimeg, R. H. Shoemaker, G. Melillo, Hypoxic induction of an HIF-1α-dependent bFGF autocrine loop drives angiogenesis in human endothelial cells. *Blood* **107**, 2705–2712 (2006).
32. T. Q. Huang *et al*., Deletion of HIF-1α partially rescues the abnormal hyaloid vascular system in Cited2 conditional knockout mouse eyes. *Mol. Vis.* **18**, 1260–1270 (2012).
33. Y. Chen *et al*., Cited2 is required for the proper formation of the hyaloid vasculature and for lens morphogenesis. *Development* **135**, 2939–2948 (2008).
34. C. C. Tokunaga *et al*., Effects of anti-VEGF treatment on the recovery of the developing retina following oxygen-induced retinopathy. *Invest. Ophthalmol. Vis. Sci.* **55**, 1884–1892 (2014).
35. M. I. Dorrell *et al*., Maintaining retinal astrocytes normalizes revascularization and prevents vascular pathology associated with oxygen-induced retinopathy. *Glia* **58**, 43–54 (2010).
36. K. Manousaridis, J. Talks, Macular ischaemia: A contraindication for anti-VEGF treatment in retinal vascular disease? *Br. J. Ophthalmol.* **96**, 179–184 (2012).
37. R. L. Avery *et al*., Systemic pharmacokinetics and pharmacodynamics of intravitreal aflibercept, bevacizumab, and ranibizumab. *Retina* **37**, 1847–1858 (2017).
38. C. Y. Huang *et al*., Changes in systemic vascular endothelial growth factor levels after intravitreal injection of aflibercept in infants with retinopathy of prematurity. *Graefes Arch. Clin. Exp. Ophthalmol.* **256**, 479–487 (2018).
39. N. Ferrara, Vascular endothelial growth factor: Basic science and clinical progress. *Endocr. Rev.* **25**, 581–611 (2004).
40. M. Saint-Geniez, T. Kurihara, E. Sekiyama, A. E. Maldonado, P. A. D'Amore, An essential role for RPE-derived soluble VEGF in the maintenance of the choriocapillaris. *Proc. Natl. Acad. Sci. U.S.A.* **106**, 18751–18756 (2009).
41. T. Kurihara *et al*., Hypoxia-induced metabolic stress in retinal pigment epithelial cells is sufficient to induce photoreceptor degeneration. *eLife* **5**, e14319 (2016).
42. Y. Usui *et al*., Neurovascular crosstalk between interneurons and capillaries is required for vision. *J. Clin. Invest.* **125**, 2335–2346 (2015).
43. V. Eremina *et al*., VEGF inhibition and renal thrombotic microangiopathy. *N. Engl. J. Med.* **358**, 1129–1136 (2008).
44. T. Zhao, X. Wang, T. Xu, X. Xu, Z. Liu, Bevacizumab significantly increases the risks of hypertension and proteinuria in cancer patients: A systematic review and comprehensive meta-analysis. *Oncotarget* **8**, 51492–51506 (2017).
45. M. Totzeck, R. I. Mincu, T. Rassaf, Cardiovascular adverse events in patients with cancer treated with bevacizumab: A meta-analysis of more than 20,000 patients. *J. Am. Heart Assoc.* **6**, e006278 (2017).
46. K. G. Falavarjani, Q. D. Nguyen, Adverse events and complications associated with intravitreal injection of anti-VEGF agents: A review of literature. *Eye (Lond.)* **27**, 787–794 (2013).
47. G. L. Semenza, Pharmacologic targeting of hypoxia-inducible factors. *Annu. Rev. Pharmacol. Toxicol.* **59**, 379–403 (2019).
48. M. DeNiro, A. Al-Halafi, F. H. Al-Mohanna, O. Alsmadi, F. A. Al-Mohanna, Pleiotropic effects of YC-1 selectively inhibit pathological retinal neovascularization and promote physiological revascularization in a mouse model of oxygen-induced retinopathy. *Mol. Pharmacol.* **77**, 348–367 (2010).
49. H. An *et al*., Novel hypoxia-inducible factor 1α (HIF-1α) inhibitors for angiogenesis-related ocular diseases: Discovery of a novel scaffold via ring-truncation strategy. *J. Med. Chem.* **61**, 9266–9286 (2018).
50. Y. Miwa *et al*., Pharmacological HIF inhibition prevents retinal neovascularization with improved visual function in a murine oxygen-induced retinopathy model. *Neurochem. Int.* **128**, 21–31 (2019).
51. S. Xiao *et al*., Fully automated, deep learning segmentation of oxygen-induced retinopathy images. *JCI Insight* **2**, 97585 (2017).
52. A. Adini *et al*., Matrigel cytometry: A novel method for quantifying angiogenesis in vivo. *J. Immunol. Methods* **342**, 78–81 (2009).